

AperTO - Archivio Istituzionale Open Access dell'Università di Torino

## Chitosan crosslinked flat scaffolds for peripheral nerve regeneration

### This is the author's manuscript

*Original Citation:*

*Availability:*

This version is available <http://hdl.handle.net/2318/1625674> since 2017-02-24T11:28:18Z

*Published version:*

DOI:10.1088/1748-6041/11/4/045010

*Terms of use:*

Open Access

Anyone can freely access the full text of works made available as "Open Access". Works made available under a Creative Commons license can be used according to the terms and conditions of said license. Use of all other works requires consent of the right holder (author or publisher) if not exempted from copyright protection by the applicable law.

(Article begins on next page)



F. Fagnard<sup>1</sup>, B. Cagnard<sup>2</sup>, F. Yu<sup>3</sup>, A. Cima<sup>4</sup>, G. Chalkley<sup>5</sup>, F. Raulf<sup>6</sup>, C. Tando-Yam<sup>7</sup>, S. Grano<sup>8</sup>, A. Rahmeh<sup>9</sup>

<sup>1</sup>Department of Clinical and Biological Sciences, and Center for Regenerative Medicine

University of Turin, Regione Piemonte, 10132, Orbassano, Italy

<sup>2</sup>Regenerative Neurology, Orthopedic Department, Trauma Center Hospital (CHU), Via Bucci  
26, 41018, Italy, Italy

<sup>3</sup>Department of Mechanical and Aerospace Engineering, Politecnico di Torino, Corso Duca degli  
Abruzzi 24, 10129, Torino, Italy

Presented address:

<sup>4</sup>Department of Veterinary Sciences, University of Turin, Largo Brambilla 2, 10095 Grugliasco TO Italy

Corresponding author:

Andrea Rahmeh

Department of Clinical and Biological Sciences, University of Turin,

Regione Piemonte, Italy

10132 Orbassano (TO)

tel: +39-011-570911, fax: +39-011-561026,

E-mail: [andrea.rahmeh@unito.it](mailto:andrea.rahmeh@unito.it)

**Abstract**

Chitosan (CS) has been widely used in a variety of biomedical applications, including peripheral nerve repair. Due to its excellent biocompatibility, biodegradability, readily availability, and antibacterial activity, in this study, CS for membranes crosslinked with phosporic anhydride phosphate (DHP) alone (CS/DHP) or in association with the γ-ethylmethacryloyloxydimethylsilylchitosan (CS/GPTMS/DHP), were fabricated with a solvent casting technique. The crosslinking ratio of crosslinking agent and CS was previously selected to obtain a composite material having both adequate mechanical properties and high biocompatibility.

In vitro cytotoxicity tests showed that both CS membranes allowed cell survival and proliferation. Moreover, CS/GPTMS/DHP membranes promoted cell adhesion. Indeed, Schwann cells like morphology and aligned in the longitudinal direction to nerve growth direction.

Preliminary *in vivo* tests carried out on both types of nerve scaffolds (CS/DHP and CS/GPTMS/DHP membranes) demonstrated that potential for: (i) promoting, as a membrane, the site of nerve transfer repair by end-to-end surgery) and avoiding post-operative nerve adhesion; (ii) bridging, as a scaffold, the nerve nerve injury after a nerve peripheral nerve lesion with different sizes.

A *Long gap rat sciatic nerve* was repaired using CS/DHP and CS/GPTMS/DHP scaffolds to further investigate their ability to induce nerve regeneration *in vivo*. CS/GPTMS/DHP tubes resulted in the nerve regains during entering and, along a 12 week post-operative time of time, they detached from the distal nerve stump. On the contrary CS/DHP scaffold provided nerve fiber regeneration and functional recovery. In addition, as outcome compatibility to median nerve repaired by suture.

**Key words:** Peripheral nerve repair; regenerative; rehabilitation; chronic; Schwann cells.

### 1. Introduction

Peripheral nerve trauma due to car accidents, sport and military injuries [1] are reported to affect, annually, more than one million people worldwide.

The possibility to repair nerve function is dependent on the severity of the damage suffered. Regeneration necessary is possible only if the continuity of the nerve is maintained. In case of complete nerve transection, a surgery is required for re-establishing a continuity between the proximal end and the distal stump. Autologous nerve grafts (anastomosis) is the "gold standard" technique for repairing peripheral nerve defects and it consists in the use of healthy nerve fragments of sensory origin (usually the sural nerve) for bridging the gap [2].

However, this practice presents some disadvantages: it requires an additional incision for harvesting the healthy sensory nerve, leading to a sensory nerve deficit; yet, graft material is limited especially in case of an extended nerve lesion, to an alternative, a sensory effluents graft for nerve reconstruction has been developed [3,4]. In particular, chronic (CN) as a natural polyacetalide, has recently attracted more and more attention due to its good biocompatibility, biodegradability, non-toxicity, easily availability and simple physicochemical properties [5,6].

Recent in vitro studies revealed the capability of CN membranes as culture for neural and neuronal Schwann cell (SC) growth [7] as well as survival and differentiation of neuronal cells [8,9].

CN-based biodegradable scaffolds have been widely used for neural repair in different animal models.

[10] CN-based nerve conduits, alone or in combination with other biomaterials, have been found to bridge effectively peripheral nerve defects [11-13]. In CN nerve guides supplied with the introduction of a biodegradable CN membrane were used to reconstruct 10 mm sciatic nerve defects in adult healthy and diabetic rats, demonstrating an enhancement in functional and morphological nerve regeneration [14].

Successful nerve regeneration of long gap has also been reported when CS surface was coated with poly(vinyl alcohol) and gelatin to enhance cell adhesion[34,35] or functionalized with polyglyoxy acid [36]. Because pure CS is brittle and degrades rapidly [37,38], improved technologies and different crosslinking methods have been developed to overcome the poor mechanical strength of CS nerve guide channel under physiological conditions, which is one of the main factors limiting the CS use in clinical application for nerve repair and nerve [39].

In the present work, ionic sodium phosphate (SDP) and 2-(diethylamino)ethyl methacrylate - DHP (DEPMDS) crosslinked CS for membranes, previously characterized in terms of physicochemical, structural, morphological, mechanical properties [26], were evaluated in terms of biological properties using *in vitro* and *in vivo* tests.

*In vitro* studies on RGD-DMPT cells were performed on degradable CS based flat membranes to evaluate biocompatibility and to assess their potential applicability as nerve repair scaffold. In addition, CS flat membranes and conduits were tested *in vivo* in model of rat median nerve repair. The outcome of nerve reconstruction was assessed at 12 weeks post-implantation through a combination of functional assessment, histological and morphological investigations.

## 2. Methods

### 2.1 Membrane preparation

CS (medium molecular weight, 70%–80% deacetylization degree, Sigma Aldrich) was dissolved in acetic acid solution 0.5M at room temperature by continuous stirring to obtain a 2.5 % (w/v) solution. Crosslinked membranes were prepared according to the method previously described by Rami and colleagues [20]. In brief:

1. DSP-crosslinked samples (CS/DSP) were obtained by adding DSP (10  $\mu$ mol drop per second) to the CS solution with a concentration of 2.5 % (w/v) with respect to the actual polymer solution volume. The actual solution was kept under stirring at room temperature for about 10 minutes.

2. CS/DSP/DSP crosslinked samples (CS/GFTMR/DSP) were obtained adding GFTMR (20% (w/v)) to the CS solution. The resulting CS/GFTMR solution was kept under stirring for 1 hour followed by the dropwise addition (one drop per second) of DSP (10 (concentration 2.5 % (w/v) and maintained under continuous stirring for 10 minutes.

Finally, 10  $\mu$ l of each solution (CS/DSP and CS/GFTMR/DSP) was poured into 6 cm Petri dishes and air-dried for 48 h to obtain flat membranes. All crosslinked dried samples were dipped into deionionized water for 10 minutes and then the water pH values were measured to evaluate the presence of acidic residues.

Finally test were performed by the authors, on CS/DSP and CS/GFTMR/DSP membranes, both in dry and in wet conditions [20].

### 2.2 In vitro cell tests on CS based membranes

In vitro cell tests were performed using RBC-DHPEL exchambers on cell lines (OEC – corneal endothelial cells, C2C12, Cytotoxicity tests were carried out on both CS/DSP and CS/GFTMR/DSP while, RBC-DHPEL adhesion, proliferation and gene expression were evaluated on CS/GFTMR/DSP due to the

higher mechanical stability of the fabricated under physiological conditions and because they were considered as "the most pure" characteristics required for C5GFPN<sub>2</sub>\_DHP fabrication were the case of C5GDP<sub>2</sub> supplemented with GPTM<sub>2</sub>. Visible outgrowth of dried over single (ORG) cultured exC5GFPN<sub>2</sub>\_DHP was then examined by confocal laser microscopy.

3.1.1 *Cytotoxicity study on C5GFPN<sub>2</sub>\_DHP and C5GDP<sub>2</sub>*

The effect of the CS based material contacts was studied on MYO-DHFT, C5GDP<sub>2</sub> and C5GFPN<sub>2</sub>\_DHP samples were incubated with a 10 minutes exposure to ultraviolet (UV) irradiation (UV lamp wavelength 300 nm, Schenckstar Scientific Co., St. Martin Glass - Egypt). Material contacts were prepared by incubating both crosslinked CS based membranes in Dulbecco's Modified Eagle Medium (DMEM, Sigma Aldrich) supplemented with 100 U/ml penicillin (Sigma), 0.1 mg/ml streptomycin (Sigma), 1 mM sodium pyruvate (Sigma), 1 mM L-glutamine (Sigma) and 10% heat inactivated fetal bovine serum (FBS, Gibco Technologies) and stored at 37 °C in a humidified atmosphere of 7% CO<sub>2</sub> for 15 days. As control media, samples of culture medium were maintained in the same conditions of C5GDP<sub>2</sub> and C5GFPN<sub>2</sub>\_DHP samples and then collected after 15 days. Then, proliferation assay on the cell line was carried on using collected media. In details, MYO-DHFT cells were seeded and cultured in the previous prepared control media at a density of 2x10<sup>5</sup> cells/cm<sup>2</sup> on 96-well dishes. After 1, 3, 5, and 7 days in vitro (DIV), cells were trypsinized and counted as a Biotek's Spectrophotometer chamber. Experiments were performed as technical replicates. The values obtained from assays were analyzed, averaged and expressed as logarithmic scale of cells collected (% 80).

3.1.2 *Cell adhesion on C5GFPN<sub>2</sub>\_DHP membranes*



Immunocytochemistry analysis was performed to specifically evaluate cell adhesion and morphology. R5-DHE37 were seeded at a density of  $1.0 \times 10^5$  cells/cm<sup>2</sup> on nucleotides and control glass slides. After 24 hours of culture, culture medium was removed, substrates with attached cells were rinsed with PBS and fixed by the addition of 4% paraformaldehyde solution (PFA, Sigma-Aldrich). After 20 min the PFA was removed and each plate was washed with PBS. Fixed cells were permeabilized with 0.1% Triton X-100 and blocked with 1% Normal goat serum in 0.05M PBS, pH 7.4 for 1 h at room temperature. F-actin was detected using TRITC-conjugated phalloidin diluted 1:1000 as blocking solution (Fluorescein-Millipore) by 1 h incubation at room temperature. Following three wash steps of 5 min each, Vectashield was followed by overnight incubation with secondary mouse-anti-actin antibody (Millipore) diluted 1:200 in PBS followed by 1 h incubation with goat anti-mouse Alexa 488 secondary antibody (Invitrogen) diluted 1:200 in PBS.

A quantitative evaluation of the morphology of the cells plated on different substrates was conducted, taking into account the distance to adjacent cell edges. The value of distance to adjacent cells was expressed as a percentage of total cultured cells in each experimental group. All the fluorescently-labeled cells were examined under a LSM 510 confocal laser microscopy system (Zeiss, Jena), which incorporates two beam paths and TRAP and is equipped with an inverted Axiovert 100 M microscope.

3.3.3 Proliferation assay on CHSEFDM\_PSP membranes

R5-DHE37 cells were seeded in DMEM containing 10% FBS, at a density of  $1.5 \times 10^5$  cells/cm<sup>2</sup> on both CHSEFDM\_PSP and glass control plates (control). After 1, 3 and 5 days, culture medium was removed, substrates with attached cells were rinsed with PBS and fixed by the addition of 4% PFA. After 20 min, PFA was removed and each plate was washed with PBS. R5-DHE37 cells were rinsed with 1% crystal violet in deionized water, acid rinsed solution in 20% acetic solution, pH 9 for

[illegible]

For normalization to multiple housekeeping genes, ubiquitin gene C (UBC) and TATA-binding protein (TBP) were used. The reaction mixture of PCR included 7.5 µg forward and reverse primers, 12.5 µl SYBR Green (Life Technologies) and 5 µl cDNA. The PCR condition were as following: initial step at 95°C for 25 s, then 40 cycles at 60°C for 15 s, and 60°C for 1 min. The results were checked by gel electrophores (data not shown).

### 2.2.5. Total protein extraction, and western blot

Total protein was extracted by solubilizing cells in boiling Laemmli buffer (2.5% SDS and 0.125 M Tris-HCl, pH 6.8), followed by 5 min at 100°C. Protein concentration was determined by the method of Lowry, and equal amounts of protein (determined at 100°C in 240 mM 2-mercaptoethanol and 180 mM Tris-HCl, pH 6.8) were separated by SDS-PAGE, transferred to a HybondE-MC nitrocellulose membrane and blocked for 1 h at 37 °C in 1× TBST (530 mM NaCl, 30 mM Tris-HCl, pH 7.6), and 0.1% Tween-20, plus 5% non-fat milk. Membranes were then incubated overnight at 4 °C in primary antibody diluted in TBST plus 1% non-fat milk. The day after, they were rinsed four times with TBST for 5 min each at room temperature and incubated for 1 h at room temperature with peroxidase-labeled secondary antibody (diluted in TBST plus 1% non-fat milk). Membranes were washed 4 times, 5 min each, with

TEST at room temperature, and specific binding was detected by the enhanced chemiluminescence (ECL system) (Amersham Biosciences) using SuperSignal<sup>®</sup> (Amersham Biosciences).

Primary and secondary antibodies used are: rabbit polyclonal anti-BcE (1:500, sc-453, Santa Cruz Biotechnology, Santa Cruz, CA, USA), mouse monoclonal anti-actin (1:1000, MA316, Sigma), horseradish peroxidase (HRP) labeling anti-mouse secondary antibody (1:1000, Amersham Biosciences), sheep anti-mouse secondary antibody (1:10000, Amersham Biosciences).

**2.2.6. Bacterial outgrowth assay on CSOP/DMG\_SDP**

DMG<sup>+</sup> exptans were harvested from stable HeLa-9 cultures, weighing approximately 200 g, cultured and maintained in HeLa's nutrient medium F12 (Gibco) for 3 days under steady conditions. Bats were sacrificed by a lethal ip. Specimen of the animal + details according with the local Ethics Committee and the European Communities Council Directive 2006/08/EC. Adipose tissues were taken to minimize pain and discomfort during any eventual future exptans for animal welfare and studies.

DMG<sup>+</sup> exptans were cultured into overnight-steady co-cultures (DM Biosciences) and CSOP/DMG\_SDP for maintenance and incubated at 37 °C for 3 days. The outgrowth was allowed to 1 in the culture medium.

Exptans were incubated for 4 days in culture medium for medium DMG at 37 °C with 5% CO<sub>2</sub> supplemented with 10 ng/ml αTGF-β. After 4 days, exptans were fixed with 4% PFA for 15 minutes at room temperature. For immunofluorescence, briefly, the specimens were incubated overnight in a solution containing both anti-mouse/fluorescein (DMG) (mouse monoclonal mouse 1:200, Sigma), and anti-porcine polyclonal anti-1:1000 (Chromomax immunoreagent primary antibodies. After washing in PBS, stable immunolabeling was carried out by incubating sections for 3 h in a solution containing two secondary antibodies: anti-mouse IgG1/Cy3 (Jackson ImmunoResearch Laboratories) and anti-mouse IgG1 Alexa Fluor 488-conjugated (Molecular Probes). All samples were observed with a LSM 510

### 3.3 In vitro work on Cx36<sup>Cre</sup>DTA, DNP and Cx36<sup>Cre</sup>

All procedures were approved by the Research Committee of the University of Toronto, by the Institutional Animal Care and Use Committee of the University of Toronto, and by the Indian Ministry of Health, in accordance with the European Communities Council Directive 2003/63/EEC.

#### 3.3.1 Animals and surgery

In vivo preliminary analysis was performed under general anesthesia on 2 adult female Wistar rats, weighing approximately 200 g, in order to evaluate baseline, variability and the possibility of their use for peripheral nerve surgery. Before using Cx36<sup>Cre</sup> animals were anesthetized in 10% volatiles for 5 minutes and then a custom fixture in the range of 10–120 µm. In the first case, the Cx36<sup>Cre</sup> animals were used to wrap crushed median nerve and was closed with a suture point (Figure 1A,B). In the second set, the Cx36<sup>Cre</sup> animals were rolled up and glued with biocompatible cyanoacrylate glue to obtain 1 cm long cables (Figure 1C,D). Median nerve was transected, 3 mm of median nerve was removed and Cx36<sup>Cre</sup> and Cx36<sup>Cre</sup>DTA, DNP rats were trained holding the two nerve stumps (Figure 1E,H). Rat were inserted from inside the cranium. **Animals were sacrificed immediately after surgery.**

**Microarray, nerve regeneration assays, nerve conduction and the 10–120 µm range, Wistar rats, baseline measurement of the 10–120 µm range, Cx36<sup>Cre</sup> and Cx36<sup>Cre</sup>DTA, DNP animals, and up and down of the 10–120 µm range, and up and down of the 10–120 µm range.** The animals were divided by three experimental groups of 4 animals each for two groups, the median nerve was transected and repaired with Cx36<sup>Cre</sup> or Cx36<sup>Cre</sup>DTA, DNP animals. Median nerve repaired with nerve sutured was used as control. The surgery procedure was previously described by Tan and colleagues [21]. The sutured and





2.1.3 *Fluorescence measurement of chemical sensors*

Gripping test sections were carried out every 5 weeks until week 12. Gripping test was performed following the same procedure previously described [22] using the BS-Grip Grip Meter (Biological Instruments, Yarmou, Italy). The test is carried out by holding the test by the tail and lowering it towards the device and then, when the animal grips the grid pulling it upward until it tears its grip. When the animal tears the device it is required the animal's paws approaches the grid in a complete finger extension. The behavior records the maximum weight that the animal manages to hold up before losing the grip. Each animal was tested three times and the average value was recorded. Since measurement of animal behavior was one of the main objectives of the study, a central daily animal expenditure was designed for passive and active movement, same metabolism and joint construction, especially during early post-operative times.

2.1.4 *Immunocytochemistry and confocal laser microscopy*

From all animals, the vertebrae collected, with representative three levels, were dissected, cut and analyzed with immunofluorescence at confocal laser microscopy. Slices of 8-10 µm thick longitudinal sections were cut by a vibratome (Oxford Microtechniques, Oxford, Germany). Sections were then incubated overnight in a solution containing anti-neurofilament 200kDa primary antibody (cytoskeletal marker, which recognizes the 200 kDa subunit of neurofilaments, dilution 1:200, Sigma) and then after washing in PBS, incubated for 3 hour in a solution containing Alexa488 conjugated anti-mouse IgG1 solution 1:200. LBA techniques. The sections were finally fluorescent with a Nikon fluorescence mounting medium and analyzed by a 1,000 X oil-coated of laser microscopy system (Nikon, Japan, Germany).

2.1.4 *Spinal cord histology and electron microscopy*



After the 12-week following this outbreak were culminated and the nerve segment fixed in the osmium was collected, fixed, and prepared for design-based morphological analysis of myelinated nerve fibers and for electron microscopy. Nerve samples were fixed by immersion immersion in 2.5% perfused glutaraldehyde and 0.5% osmium in 0.1 M Hanesen phosphate buffer for 4 h. Nerve segments were then washed in a solution containing 0.5% osmium in 0.1 M Hanesen phosphate buffer, post-fixed in 1% osmium tetroxide, dehydrated and embedded in araldite. From each nerve, series of semi-thin transverse sections (2.5 µm thickness) were cut starting from the distal stump of each median nerve specimen, using an Ultramicrotome (Leica Microsystems, Wetzlar, Germany) and stained using Toluidine blue for high resolution light microscopy examination and design-based morphology. For transmission electron microscopy, ultrathin sections (50-90 nm thick) were cut using the same ultramicrotome and stained with osmium tetroxide solution of osmium tetroxide and lead citrate. Ultra-thin sections were analyzed using a JEOL 1010 transmission electron microscope (JEOL, Tokyo, Japan).

### 2.3.1 design-based quantitative morphology of nerve fiber representation

In each nerve segment that contained a CNFMP lesion, design-based morphological analysis was carried out using one randomly selected relative thin stained transverse section. A DM6000B microscope equipped with a DPC720 digital camera and an SEMV image manager system (Leica Microsystems, Wetzlar, Germany) was used for microscopy. The final magnification was 600X, enabling us to carry out qualitative and quantitative analysis of myelinated nerve fibers. One area thin section from each nerve was randomly selected and the total cross-sectional area of the nerve was measured. The sample of these in each nerve was then randomly selected using a previously described stereological method [25]. Two-dimensional director profiles were also used to select an unbiased representative sample of myelinated nerve fibers. Fiber number was calculated both fiber and cross

area were measured and the circle fitting diameter of fiber (D) and area (A) were calculated. These data were used to calculate specific thickness (D/A) and the g-value (D/A).

3.4 Statistics

For in vivo experiments, data were expressed as mean  $\pm$  SEM. Statistical analysis was carried out using single factor analysis of variance (ANOVA) post hoc Bonferroni. Values of \*p<0.05, \*\*p<0.01, \*\*\*p<0.001 were considered as statistically significant. For in vitro experiments data were expressed as mean  $\pm$  SD. Statistical analysis was carried out using Two-sample t-Test. Values of \*p<0.05, \*\*p<0.01, \*\*\*p<0.001.

3. Results

3.1 In vitro cell lines as CS hard template

3.1.1 - Cytotoxicity study on C5GFTM, DHP and C5BAP

The effect of the CS based nanoscale carbon was studied by RTG-23077 proliferation assay counting the number of proliferating cells after 2, 5, 7, 9 and 10 days (Figure 1). RTG-23077 showed the survival of C5BAP and C5GFTM, DHP showed no cytotoxic effect since no significant differences in cell number were detected between these two culture conditions and the control.

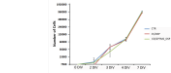


Figure 1. Evaluation of the effect of disulfide gradient. Representative graph of R19-DRD77 cell adhesion to CS/GPTMS-DSF and CS/GPTMS-DSF+DSF substrates.

#### 4.1.2 Cell adhesion on CS/GPTMS-DSF substrates

R19-DRD77 cells were seeded on CS/GPTMS-DSF and on control glass. Immunocytochemistry analysis was performed after 24 hours of culture to specifically evaluate cell adhesion and morphology. In order to obtain a more detailed evaluation of cell adhesion, the cells cytoskeleton and focal adhesion complex were stained using TRITC-conjugated phalloidin and anti- $\alpha$ -tubulin antibody, respectively. R19-DRD77 cells, internalized and integrated well with CS/GPTMS-DSF substrates. Differences in morphology and size were observed when R19-DRD77 cells were cultured on control glass and CS/GPTMS-DSF (Figure 1). Cells on control glass displayed a higher size; they were also more spread without particular orientation of the actin cytoskeleton (Figure 1A and C). Cells cultured on CS/GPTMS-DSF displayed a more elongated morphology characterized by a typical oval shaped cell body with long extensions, giving an overall spindle shape that is typical of MCs (Figure 1B and D). The analysis of the morphology of these cells plated on different substrates showed that the cells of cells plated on control substrates (glass) presented a flattened form, similarly to fibroblasts, and only

DN, an elongated shape similar to SC. By contrast, 65% of the cells cultured on CS-GPTM<sub>2</sub>\_DHP had presented the SC-like elongated shape.

Viability immunostaining was performed to visualize the exact location of focal adhesion sites.

Viability-positive sites were observed on cells seeded both on control and CS-GPTM<sub>2</sub>\_DHP, but with different distributions. CS-GPTM<sub>2</sub>\_DHP scaffolds were populated with a higher concentration of viabilities around the surface (Figure 3C), while protein accumulation at the edges of cells was mainly observed in control (Figure 3D).

#### 3.3.3 Proliferation assay on CS-GPTM<sub>2</sub>\_DHP scaffolds

Proliferation assay was performed on CS-GPTM<sub>2</sub>\_DHP samples (Figure 3E). R1A-DMSO cells were cultured on both CS-GPTM<sub>2</sub>\_DHP and glass plates (control). The number of proliferating cells was determined after 1, 3 and 4 DIV.

R1A-DMSO cells seeded on CS-GPTM<sub>2</sub>\_DHP showed lower proliferation rates and significant differences in cell numbers were detected in this culture condition after 3 DIV (\*\*p<0.01) and 4 DIV (\*\*p<0.001), in comparison to practice control. Yet, it was possible to observe a constant increase of cell numbers on CS-GPTM<sub>2</sub>\_DHP samples at each time point.

#### 3.3.4 Gene and protein expression of R1A-DMSO cultured on CS-GPTM<sub>2</sub>\_DHP samples

Bas, Bcl2, pERK and SIRT mRNA expression changes were evaluated in early progenitors and cell survival signaling after 1 and 4 days of culture of R1A-DMSO cells on CS-GPTM<sub>2</sub>\_DHP samples.

The relative values of Bas, pERK and SIRT mRNA expression rates are significantly different when comparing CS-GPTM<sub>2</sub>\_DHP with control conditions, both after 3 and 4 days of culture. (Data not shown). By contrast, significant differences in the Bcl2 mRNA expression was observed after 3 days of



3.1.3. *Neuron outgrowth assays on CS/GFBN\_HSP*

DIC-Optikon was harvested from adult female Wistar rats and cultured for 4 days on micro-patterned coverslips and CS/GFBN\_HSP for neurite outgrowth. The cultures were fixed and immunostained for NF-200kDa (green) and propidium iodide and then analyzed by laser confocal microscopy. A double labeling immunofluorescence revealed that both neuronal intermediates (neurite protrusion) were supported by DMSO neurons (Figure 9).

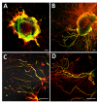


**Figure 9.** Fluorescence microscopy images of neural outgrowth at 4 days after DMSO exposure. CS/GFBN\_HSP coverslips (A, C) and CS/GFBN\_HSP coverslips (B, D) were used. CS/GFBN\_HSP coverslips were used as a control. Scale bar: 100 µm.

3.2. *In vitro patch-clamp analysis*

In order to evaluate membraneability for peripheral nerve surgery, the membranes of CS/GFBN\_HSP were tested in vitro in adult female Wistar rats.

Both membranes were to be immersed in PBS buffer in order to make them softer. The pipette can adapt size and shape of membranes depending on the size of the nerve and the technique used. They can be used to perform peripheral nerve transection (Figure 10) or to conduct to bridge a nerve defect (Figure 10). Both membranes resulted in a good membraneability after the PBS immersion.

and they are easy to use with a single, or multiple, procedures for appropriate use, and they are easily added or updated about CKOP/DH, DSP available to much more easily.

### 3.3.3. Inclusion with CKOP/DH, DSP and CKOP/DH modules

#### 3.3.3.1. Experimental assessment of functional recovery

In this series of experiments, the same control was used with both CKOP/DH and CKOP/DH, DSP modules. The measured outcome measures of function were not repeated by either up and side shaped CKOP/DH or CKOP/DH, DSP modules. Repeated assessment was not (although) repeat was used as control.

Figure 5 reports the post-operative time course of functional recovery for rats treated using CKOP/DH and endogenous graft. In the group of CKOP/DH, DSP modules, functional recovery of finger flexor muscle activity occurred during a post-operative period. This observed to be due to the detection of CKOP/DH, DSP after the initial recovery.

The function of finger flexor muscle, measured by the motion were noted to recover faster for endogenous muscle a performance markedly different from CKOP/DH at week 4 after lesion ( $p < 0.05$ ). Functional recovery for CKOP/DH noted at week 4 and progressively increased. At week 9 and 12, no more significant differences were detectable between original and CKOP/DH treatment.

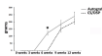


**Figure 5. Post-operative time course of functional recovery.** Line graph showing the post-operative time course of functional recovery for endogenous muscle a performance markedly different from CKOP/DH at week 4 after lesion ( $p < 0.05$ ). Functional recovery for CKOP/DH noted at week 4 and progressively increased. At week 9 and 12, no more significant differences were detectable between original and CKOP/DH treatment.

3.1.2 Immunocytochemistry and confocal laser microscopy

Axonal regeneration was analyzed by confocal laser microscopy on longitudinal nerve tissue sections after nerve/blastema rejoining (Figure 6). After 12 weeks post injury, the axons, segments of both Cx36P308, DHP and Cx36P308 control (Figures 6F) positive staining for axons, while distended and straight extensions in the Cx36P308, DHP control (Figure 6E) and linearly oriented in Cx36P308 control (Figure 6E).



Figure 6: The axon distal segment evaluation. Transverse sections are longitudinal sections of 12 weeks control and Cx36P308, DHP nerve joined proximal and nerve Cx36P308, DHP distal axons that were highly positively stained and distended (A), while properly linearly aligned (B) axons were found in Cx36P308, DHP nerve (C).

3.1.3 Light and transmission electron microscope analysis

Figure 7 shows high-resolution light and transmission electron microscope images of the distal axonal nerve segment, repaired with untreated or Cx36P308 control and harvested at 12 weeks post operation. Distal axonal nerve joined with Cx36P308, DHP nerve and proximal nerve axons were found to be detached from the distal segment (A). Small myelinated axons and microvasculature typical of regenerated nerve fibers were detected both in nerves repaired with untreated (Figure 7 A,C,E,G) and with Cx36P308 control (Figure 7B,D,F,H).



Moreover, translocation electron microscopy showed many small vesicles (less than 100 nm) stages of replication (Figure 7E,F) as well as unreplicated DNA (Figure 7G,H), in vesicles before replication with CS-DSP coated and without.

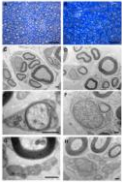


**Figure 7. Replicated vesicles.** Cryo-electron tomograms of vesicles before and after replication in the presence of CS-DSP coated and without. (A) Cryo-EM tomogram of a vesicle before replication. (B) Cryo-EM tomogram of a vesicle after replication. (C) Cryo-EM tomogram of a vesicle before replication. (D) Cryo-EM tomogram of a vesicle after replication. (E) Cryo-EM tomogram of a vesicle before replication. (F) Cryo-EM tomogram of a vesicle after replication. (G) Cryo-EM tomogram of a vesicle before replication. (H) Cryo-EM tomogram of a vesicle after replication.

2.1.4 Bridge-based quantitative monitoring of nerve fiber regeneration

12-week post injury, bridge-based morphological analysis of regenerated axons was repeated with CSFDP values or averaged dorsal-ventral axonal counts in some of total number of explanted fibers (average = 4000-1000). CSFDP = 7000-1000. Axon and fiber diameters and Grains was significantly lower ( $p < 0.05$ ) in axons versus control with CSFDP values when compared to axons, while myelin thickness dorsal-ventral axonal counts (Figure 6).

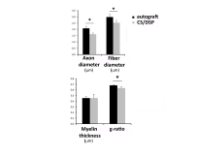


Figure 6. Morphometrical analysis of regenerating fibers. Bar charts representing morphological parameters of regenerated axons. Data are represented as mean  $\pm$  SD. Significant differences between the control and CSFDP values were observed at  $p < 0.05$ . Significant differences between the control and CSFDP values were observed at  $p < 0.05$ .

#### 4. Discussion

Application of CS in tissue engineering is a well-known and exciting topic [14,15]. This biomaterial's attractive not only for the high biocompatibility and biodegradability, but also for the anisotropic properties and the absence of immune responses.

However, physical and mechanical features of CS when it is associated with aqueous solution have to be carefully considered in order to apply it properly for regenerative purposes.

In this manuscript CS was treated with crosslinking agent able to act on its chemical physical and mechanical properties, mainly  $\gamma$ -phosphorylethylmethacrylate (GPTMA), dibasic sodium phosphate (DSP) and a combination of GPTMA and DSP (GPTMA\_DSP), as previously described by Bortolotto and colleagues [35].

**The present use of GPTMA allowed that others agent was homogeneously distributed in the developed**

**membranes and achieved the water stability and the release of CS/GPTMA\_DSP membranes**

**against CS/DSP samples.**

Both CS/GPTMA\_DSP and CS/DSP for membranes were studied in vitro and in vivo for the implementation of CS-based nerve scaffolds.

First of all, the presence of degradation of the CS membranes, both CS/DSP and CS/GPTMA\_DSP, showed no negative effects on physical, chemical and performance.

Via proliferation analysis of glial cells seeded on CS/GPTMA\_DSP membranes led to confirm that CS

is capable to support glial cell proliferation [35] although delayed in comparison to positive control.

This is attributable to the need for an initial adjustment in the new culture. The need of adaptation of the cells to the culture new dimensional site by gene expression analysis of the cell specific gene.

It is clear that is significantly lower in each gene after 5 days on CS/GPTMA\_DSP while the difference was no more detectable after 6 days.

The analysis of cell cultures in the CxGPTM<sub>2</sub>NSP neurons showed that glia cells displayed a different morphology and axon and dendrite distribution, supporting the view that they have a higher migration capacity on the biomaterial, a key requirement for the early stages of nerve regeneration [24]. The axon cytoskeleton is a highly dynamic network composed of actin polymer and a large variety of associated proteins. The function of the axon cytoskeleton is to maintain a variety of essential biological functions, including intracellular and extracellular movement and structural support. The orientation and distribution of axon filaments within a cell is, therefore, an important determinant of cellular shape, adhesion and motility [25].

The movement of the neurites of neurons with the material represents a key preliminary step to evaluate, in vivo, the potential for neural regeneration. Explan of neuronal morphology (RNG) are a valuable in vivo model to observe the neurite adaptation to different substrates [26]. In our research, while RNG was cultured on CxGPTM<sub>2</sub>NSP substrates and on glass, as control. After two days a high number of neurites sprouting from the surface of both control and nerve axons, was appreciated on both substrates. Although quantitative analysis was not carried out, careful observation led to detect a greater sprouting and neurite extension on the C3 substrate in comparison to control.

In preparation of in vivo experiments, a series of preliminary work allowed us to evaluate the neurocompatibility of C3 membranes. It was possible to establish the easy handling and the possibility to build, at the time of the surgery, a tube of specific size and shape depending on the extent of nerve damage, although it was evident that the CxGPTM<sub>2</sub>NSP is much more flexible in comparison with C3NSP.

Both CxNSP and CxGPTM<sub>2</sub>NSP materials were used for bridging nerves 10 mm long rat median nerve defects, and the outcome of 12 weeks post-implantation was evaluated by functional, immunohistochemical and histological investigation. We observed that CxGPTM<sub>2</sub>NSP tubes were detached from the distal sensory rim, due to excessive flexibility, and then an functional recovery [27].

combined. This work was confirmed by confocal laser microscopy which displayed very poor axonal regeneration with no synaptic transmission inside Cx36PDB<sub>1</sub>30P conductors.

By contrast, Cx36SP conductors showed functional recovery that started at week 4 and progressively increased reaching values similar to unoperated already at week 5. The delayed functional recovery is justified by the different repair technique and it is in line with the results obtained using other types of conductors [26].

Interestingly, morphological analysis showed structures similar to those typical of regenerated nerve fibers with small nerve fibers in different myelination stages and myelinated fibers. Thus, though morphological analysis revealed that Cx36SP have, on average, smaller fibers than unoperated.

#### 5. Conclusions

In this work, we have evaluated a functional axonal electron transfer of the conductors biocompatibility, biodegradability, axonal conductivity, and adhesion activity. Considering previous low potential, electron with adequate mechanical properties for successful application in the field of peripheral nerve regeneration.

The experiment showed that Cx36SP conductors promote peripheral nerve regeneration with an electron flow in that matched by nerve conduction which was previously considered as the gold standard for treating severe nerve deficits. These newly developed nerve guides should thus be regarded as promising alternatives to traditional nerve conduits.

However, it could be future the combination of different materials with filling materials conjugated with growth factors [26] might be able to further increase the effectiveness of the medical device. Yet, creation of a 3D inner structure, which simulates extracellular matrix, might also provide a further support to axon and glial cells [23,22,23]. Therefore, although the device that we propose is simple

and may be applied during surgery. Future experiments should clearly evaluate the functionalization of the scaffolded fibrous tubes and further increase the regenerative potential of the device.

**Acknowledgments**

This research was supported by Regione Piemonte - P.O.R. di Innovazione - MICROSAFE project (number 130/2013).  
The authors declare no conflict of interest.

## References

- [illegible]

15. Cheng SH, Zhang J, Yang Q, Cheng Y, Zhou Y, et al. (2005) Ionic cytoplasmic properties and nerve excitability of myelinated fibers from chronic and genetic leukodystrophies. *Neuroscience* 134: 1017–1030.

16. Wang X, Hu W, Cao Y, Sun Y, Wu L, et al. (2005) Drug sodium nerve regeneration across a 30 mm distance bridged by a collagen/chitosan conductive gel. *Biomaterials* 26: 1597–1605.

17. Wang X, Hu W, Wu Y, Cheng Y, Sun Y, et al. (2007) Physical properties and biocompatibility of a porous collagen/chitosan fiber engineered conduit for nerve regeneration. *Biomaterials* 28: 20–28.

18. Yang X, Gu X, Sun B, Hu W, Wang X, et al. (2006) Efficacy and properties of a porous collagen/chitosan fiber for nerve regeneration. *Biomaterials* 27: 1717–1727.

19. An G, Jiang YN, Sun HJ, Guo J, Zhu WC, et al. (2011) The regeneration of neuronal axons across an adult rat spinal cord transected conduit with bone matrix, collagen, and laminated polyethylene glycol-coated chitosan. *Biomaterials* 32: 792–798.

20. Ruan F, Ruan J, Tang C, Chen Y, Guo H, et al. (2015) Clinical outcomes for nerve engineering: regeneration of ulnar nerve. *Biomaterials* 36: 30–38.

21. Sun F, Bian W, Li Wenhua S, Anshun C, Kunitomo S, et al. (2008) Engineering of the mouse spinal nerve conduit for the experimental assessment of peripheral nerve regeneration. *J Neurosci Methods* 169: 159–177.

22. Li F, Kishida T, Cheng Y, Li X, Liang Y, Liang Y, et al. (2008) Chapter 6 Methods and protocols in peripheral nerve regeneration experimental research part 1 experimental models. In: *Rev Neurobiol* 147: 47–70.

23. Kishida T, Chen Y, Kunitomo S, Li X, Liang Y, et al. (2010) Evaluation of the neuroregenerative abilities of the superior of myelinated axons in the rat sciatic nerve: a multicenter study. *J Neurocytol* 39: 547–56.

24. Nannmark UH, Papp HO, Wernberg L, Rasmus M, Ruan F (2008) Chondroitinase based up collagen and laminated poly glycol chitosan engineered. *Int J Biol Cell Res* 1(1): 147–151.

25. Li G, Zhou X, Zhou W, Zhang X, Wang C, et al. (2010) Porous chitosan scaffold with surface micropattern and inner porosity and their effect on Schwann cells. *Biomaterials* 31: 4312–4321.

26. Chen YP, McDonald D, Cheng C, Wagnon M, Bryant J, et al. (2005) Axon and Schwann cell guidance using novel materials. *Neuroscience* 134: 111–121.

27. Johnson ME, Kung ME, Anshun SH, Ruan FJ, Sun H, et al. (2011) F-actin bundles direct the axonal outgrowth of Schwann cells through cell-based tissue engineering. *J Cell Biol* 194: 441–451.

28. Chen X, Kunitomo S, Fugusawa J, Ruan J, Kishida T, Goshima C (2004) In vivo models for peripheral nerve regeneration. *Int J Neurosci* 114: 387–396.

29. Goshima C, Patel D, Bian W, Goshima C, Mungai M, Ruan FJ, et al. (2005) Axonal delivery of the Schwann cell myelin protein (SCMP) has a positive effect on regenerated nerve fiber maturation. *Gene Ther* 22: 901–907.



20. Mounier, A.R.; Winkler, C.; Dingemans, P.; Janssen, C.; Buijs, A., et al. (2014) Neurotechnology across time: *From the laboratory to the clinic*. *Neuroscience & Biomedicine* 9, 1-10.
21. Green, S.; Green, S.; Patterson, C.; De R. Battista, R. (2013) From engineering and peripheral nerve regeneration to medicine. *Ann. Rev. Neurosci.* 36, 15-35.
22. Green, S.; Patterson, M.R.; Battista, R.; C. Battista, R.; Green, S., et al. The influence of electrode design on the behavior of peripheral nerve regeneration. *Neuro. Sci. Lett.* 4, 100-105.
23. de Rubeis, G.F.; Mounier, A.R.; Battista, R.; Battista, R.; Battista, R. (2015) Designing ideal electrodes for peripheral nerve repair. *Neurosci. Biomedicine* 10, 1-10.